

GSDeformer: Direct Cage-based Deformation for 3D Gaussian Splatting

JIAJUN HUANG, Bournemouth University, United Kingdom

HONGCHUAN YU, Bournemouth University, United Kingdom

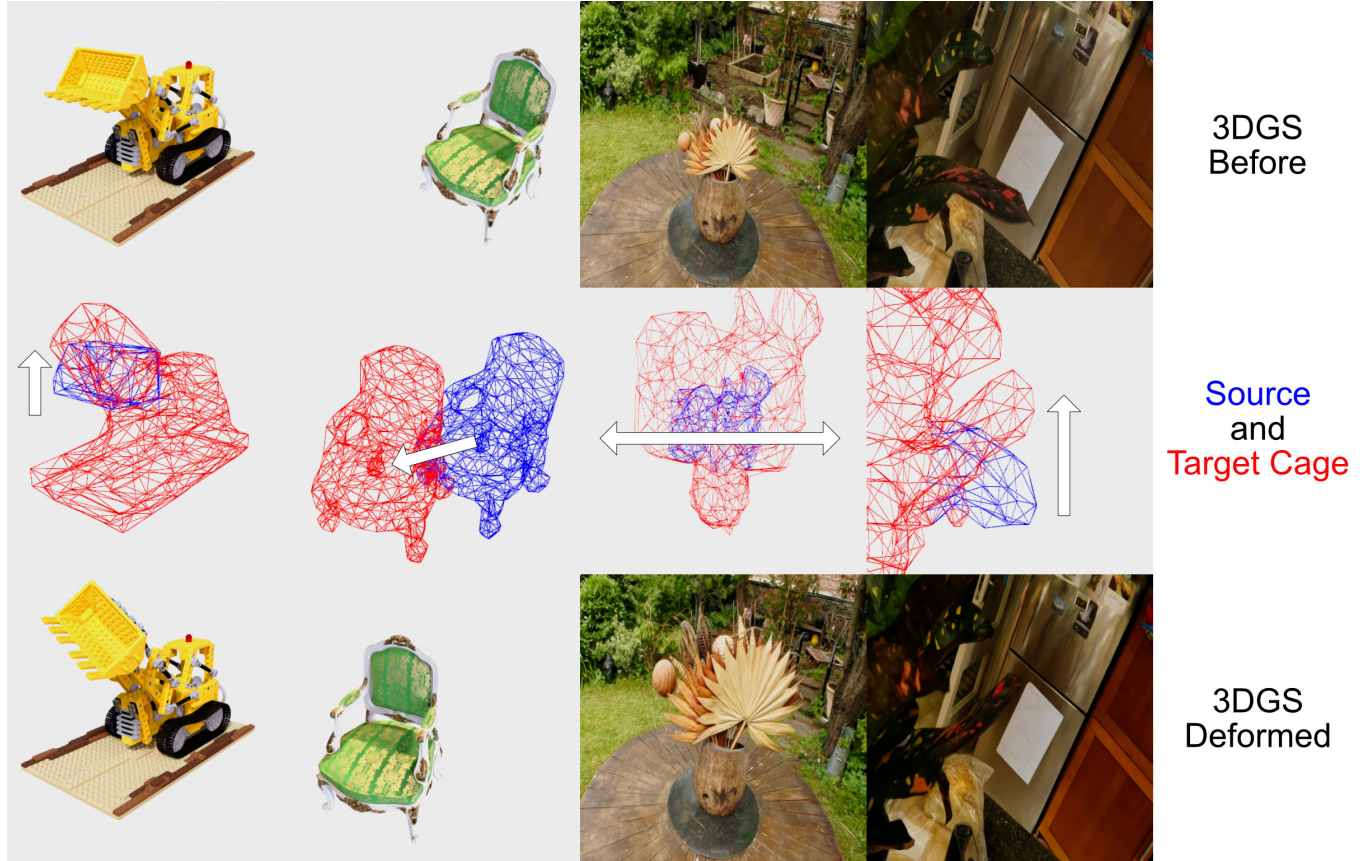


Fig. 1. Applying our method to both synthetic and real-world scenes. As can be seen, our method can perform various forms of deformation with high quality, such as twisting the blade of the bulldozer, moving the chair, expanding the flowers on the vase or lifting the leaves of the plant. Please refer to our project site for more results.

We present GSDeformer, a method that achieves free-form deformation on 3D Gaussian Splatting(3DGS) without requiring any architectural changes. Our method extends cage-based deformation, a traditional mesh deformation method, to 3DGS. This is done by converting 3DGS into a novel proxy point cloud representation, where its deformation can be used to infer the transformations to apply on the 3D gaussians making up 3DGS. We also propose an automatic cage construction algorithm for 3DGS to minimize manual work. Our method does not modify the underlying architecture of 3DGS. Therefore, any existing trained vanilla 3DGS can be easily edited by our method. We compare the deformation capability of our method against other existing methods, demonstrating the ease of use and comparable quality of our method, despite being more direct and thus easier to integrate with other concurrent developments on 3DGS. Project Page: <https://jhuangbu.github.io/gsdeformer/>

Authors' addresses: Jiajun Huang, jhuang@bournemouth.ac.uk, Bournemouth University, Bournemouth, United Kingdom; Hongchuan Yu, hyu@bournemouth.ac.uk, Bournemouth University, Bournemouth, United Kingdom.

CCS Concepts: • **Computing methodologies** → **Computer vision tasks; Shape modeling**; *Shape representations*.

Additional Key Words and Phrases: Scene Representation, Radiance Field, Scene Manipulation, Cage-based Deformation, Free-form Deformation

1 INTRODUCTION

Radiance field-based scene representations, especially 3D Gaussian Splatting(3DGS)[Kerbl et al. 2023], have achieved remarkable quality in capturing and representing real-life scenes. However, for this representation to be usable for practical downstream applications such as animation, virtual reality or augmented reality, the user should be able to manipulate the captured scene for privacy or artistic purposes. Namely, the user should be able to easily and freely manipulate the captured scene.

However, existing methods do not provide free-form manipulation, namely deformation, of 3DGS. Work that achieves deformation on Neural Radiance Fields[Mildenhall et al. 2020], such as DeformingNeRF[Xu and Harada 2022] and NeRFShop[Jambon et al. 2023] builds upon volumetric rendering, a process that 3DGS does not employ. Work that enables deformation on 3DGS, such as GaMeS[Waczyńska et al. 2024], Gaussian Frosting[Guédon and Lepetit 2024] or SC-GS[Huang et al. 2023], requires non-trivial extensions to the 3DGS representation or additional data. This makes editing existing trained 3DGS or integrating them with other work on 3DGS difficult.

Aiming to overcome these challenges, we propose GSDeformer, a method that achieves free-form manipulation of 3DGS that can be easily applied to any trained 3DGS without extensive conversion or re-training. Our work is based on Cage-based Deformation(CBD), which deforms a fine mesh and points inside it according to the deformation of a coarse mesh. The coarse mesh is called a cage and is more intuitive for the user to edit. In this work, we derive a novel approach that converts the gaussians making up the 3DGS representation into a point cloud, which can be deformed by cage-based deformation. We then use the deformation of the proxy point cloud to infer the transformation of the gaussians. The cage used for deformation can be created manually or with our automated cage construction algorithm. Our direct approach towards transformation allows us to perform deformations of any trained vanilla 3DGS without extensive retraining or conversion. Making our method easier to integrate with other methods.

We showcase our method’s editing ability by testing it on several synthetic and real-world scenes. Results show that our cage-building method produces easy-to-use proxy meshes, while our deformation algorithm archives deformation and manipulation of 3DGS with quality comparable to or even superseding methods that require architecture modifications.

In summary, our contributions are:

- We propose GSDeformer, which, to the best of our knowledge, is the first method that achieves free-form deformation on 3D Gaussian Splatting without changes to its underlying architecture nor requiring additional data.
- We also propose an automatic cage construction algorithm for 3DGS for building cages for manipulation
- We conduct extensive experiments to showcase our method’s ease of use and competitive result quality against existing methods despite being simpler and having fewer requirements.

2 RELATED WORK

2.1 Editing 3D Gaussian Splatting Scenes

Numerous works have been proposed to achieve editing on 3D Gaussian Splatting(3DGS). This includes high-level textual prompt-driven editing, such as GaussianEditor[Chen et al. 2023], VcEdit[Wang et al. 2024] and GaussCtrl[Wu et al. 2024], as well as other lower-level, more explicit editing methods.

To enable low-level, explicit editing, one well-explored avenue is binding the Gaussian distributions making up the representation

onto a mesh surface. Deforming 3DGS is then achieved by deforming the proxy mesh. This line of work is pioneered by SuGaR[Guédon and Lepetit 2023] and further developed by GaussianFrosting[Guédon and Lepetit 2024], GaMeS[Waczyńska et al. 2024] and Gao et al.[Gao et al. 2024]. SuGaR proposes a mesh extraction method that produces mesh from 3DGS, along with a set of training regularizations that improve the quality of the mesh extracted from it. GaussianFrosting builds upon SuGaR by proposing a more flexible formulation to bind the distributions onto the mesh. GaMeS and Gao et al. build their representation based on a provided initial mesh and perform further training based on it.

Despite achieving great results, the main limitation of the mesh-bounding methods is that they alter the architecture of 3DGS to achieve deformation, requiring costly retraining and even the initial mesh provided to them. These architectural modifications or data requirements make editing existing learned 3DGS scenes impossible and lead to harder integration with other concurrent developments on 3DGS.

Another branch of work builds upon control points, SC-GS[Huang et al. 2023] proposes to deform gaussians by transferring the movement of control points. The control points and weights on gaussians for transfer are learned from videos. This dependency on video data makes this method limiting as well.

In addition to the approaches above, physics simulations has also been proposed to achieve manipulation of 3DGS. PhysGaussian[Xie et al. 2023] leverages the point cloud nature of 3DGS to integrate with Material Point Method[Jiang et al. 2016] dynamics, creating plausible object deformations on touch or push. Gaussian Splashing[Feng et al. 2024] combines 3DGS and position-based dynamics (PBD) [Macklin et al. 2016] for simulation. Spring-Gaus[Zhong et al. 2024] combines the Spring-Mass model into the architecture of dynamic 3DGS and learns the physical properties like mass and velocity from videos. PhysDreamer[Zhang et al. 2024] further develops this idea by learning from dynamic videos generated by Stable Videdo Diffusion[Blattmann et al. 2023]. Feature Splatting[Qiu et al. 2024] further incorporates semantic priors from other models and makes object-level simulation possible. However, these methods are more focused on intuitive interaction rather than fully controllable, detailed editing for object deformation and manipulation.

In contrast, our method builds upon cage-based deformation, where the cage can be generated automatically from a trained 3DGS representation. As presented in Figure 4 and Table 1, Our method (1) achieves fully controllable, detailed deformation (2) does not require any video data for achieving deformation (3) achieves comparable deformation quality against mesh-bounding methods without intrusive architecture modifications. Not changing architecture allows our method to easily edit any existing trained 3DGS representation.

2.2 Cage-based Deformation

Cage-based deformation(CBD) is a family of methods that deforms a fine mesh (or space inside it) according to the deformation of a coarse mesh that approximates the fine mesh (called cage). This is done by transforming the space inside the cage and applying such transformation to the mesh vertices.

The core of cage-based deformation is the formulation of cage coordinates, which is used to represent the positions of points inside the cage w.r.t. the cage vertices. Previous work has proposed several kinds of cage coordinates and achieved promising results on mesh deformation. Examples include mean value coordinates (MVC)[Floater 2003][Ju et al. 2005b], harmonic coordinates (HC)[DeRose and Meyer 2006][Joshi et al. 2007] and green coordinates (GC)[Lipman et al. 2008].

Several methods have been proposed to extend cage-based deformation to radiance field-based scene representations, such as DeformingNeRF[Xu and Harada 2022], NeRFShop[Jambon et al. 2023] or Li et al.[Li and Pan 2023]. However, those works perform deformation by creating a deformation field to deform the sample points on rays shot during volumetric rendering. This cannot be trivially extended to 3DGS as 3DGS uses rasterization for rendering instead.

For cage generation, NeRFShop[Jambon et al. 2023] proposes to use marching cubes to generate meshes and decimate it using edge collapse[Garland and Heckbert 1997]. DeformingNeRF[Xu and Harada 2022] generates mesh using marching cube as well, but it then converts it to the cage using Xian et al. [Xian et al. 2009], where it converts the mesh into a coarse voxel field, and then extracts and smooth the field surface into cage mesh. In contrast, our method builds upon Bounding Proxy [Calderon and Boubekeur 2017], a more advanced cage construction method that provides fine-grained level-of-detail control. Our approach directly converts the density field represented by 3DGS into the final voxel grid for processing, which is simpler and more efficient.

3 METHOD

3.1 Preliminaries

We precede the detailed description of our algorithm by quickly revisiting the design of 3D Gaussian Splatting and cage-based deformation methods.

3D Gaussian Splatting 3D Gaussian Splatting(3DGS)[Kerbl et al. 2023] is an explicit scene representation that represents a 3D scene using a collection of 3D gaussian distributions. Each distribution has mean $\mu \in \mathbb{R}^3$, covariance $\Sigma \in \mathbb{M}^{3 \times 3}$, opacity $\alpha \in \mathbb{R}$ and spherical harmonics parameters $C \in \mathbb{R}^k$ (k is the degrees of freedom) for modelling view-dependent colour. The covariance matrix is further decomposed into a rotation matrix R (encoded as quaternion) and a scaling matrix S (encoded as scaling vector) via $\Sigma = RSSR^T$.

The architecture of 3DGS, namely representing scenes using a collection of 3D ellipsoids encoded as 3D Gaussian distributions, is the key motivator of our method.

Cage-based Deformation To deform a fine mesh with a cage, given a cage C_s with vertices $\{v_j\}$. The position of points $\mathbf{x} \in \mathbb{R}^3$ inside C_s can be represented using cage coordinates $\{\omega_j\}$ (such as mean value coordinate[Ju et al. 2005a]), which represent the position of \mathbf{x} relative to vertices of C_s . Formally, the position of \mathbf{x} is the weighted sum of the position of cage vertices:

$$\mathbf{x} = \sum_j \omega_j(\mathbf{x}) \mathbf{v}_j. \quad (1)$$

After the cage is deformed from C_s to C_d with vertices $\{v_{dj}\}$. With the calculated cage coordinates, the deformed position of \mathbf{x} for the deformed cage C_d can be calculated:

$$\mathbf{x}' = \sum_j \omega_j(\mathbf{x}) \mathbf{v}_{dj}. \quad (2)$$

As the cage encompasses the fine mesh, the fine mesh can be deformed by deforming its vertices. This method also applies to any points inside the cage.

3.2 Cage-Building Algorithm

Based on the framework of Bounding Proxy[Calderon and Boubekeur 2017], given a trained 3DGS scene representation \mathcal{S}_s , we aim to construct a coarse cage C_s that encompasses it. The coarse cage can then be edited.

As shown in the left side of Figure 2, we start by converting the 3DGS representation into a binary occupancy voxel grid. This is done by comparing the density value of every voxel against a threshold value, where voxels with values above the threshold are set to one, and others are set to zero. The density value is defined to be the sum of the voxel center’s opacity $d(\mathbf{v})$ w.r.t the K -closest 3D gaussians:

$$d(\mathbf{v}) = \sum_g \alpha_g \exp\left(-\frac{1}{2}(\mathbf{p} - \mu_g)^T \Sigma_g^{-1}(\mathbf{p} - \mu_g)\right) \quad (3)$$

where g are the gaussians whose mean is K -closest to the voxel center \mathbf{v} , and $\alpha_g, \mu_g, \Sigma_g$ are their opacity, mean and covariance.

We then apply the morphological closing operator proposed by Bounding Proxy[Calderon and Boubekeur 2017] to remove details progressively.

With the processed grid, we mesh the contour of the voxel grid by marching cube, employ bilateral mesh filtering to smoothen the extracted mesh, and finally decimate the mesh to create the cage by applying a progressive edge-collapse algorithm.

3.3 Deformation Algorithm

Given a trained 3DGS scene representation \mathcal{S}_s , a source/target cage pair C_s and C_d that deforms part of or the entire scene, our method aims to produce \mathcal{S}_d , which is 3DGS with the deformation applied.

Our method performs deformation on the 3D Gaussian distributions that make up the 3DGS scene representation. More concretely, for every 3D Gaussian distribution d with mean $\mu_d \in \mathbb{R}^3$ and covariance $\Sigma_d \in \mathbb{M}^{3 \times 3}$ (encoded using rotation matrix R and scaling matrix S), we deform it using the following five steps, as presented in the right side of Figure 2. Please refer to the appendices for the pseudo-code description of our deformation algorithm.

3.3.1 Distribution to Ellipsoid. We start by creating an isocontour ellipsoid from the probability distribution function(PDF) of the 3D Gaussian distribution.

More concretely, for a 3D Gaussian distribution with mean μ_d and covariance Σ_d . It’s PDF at point \mathbf{x} is:

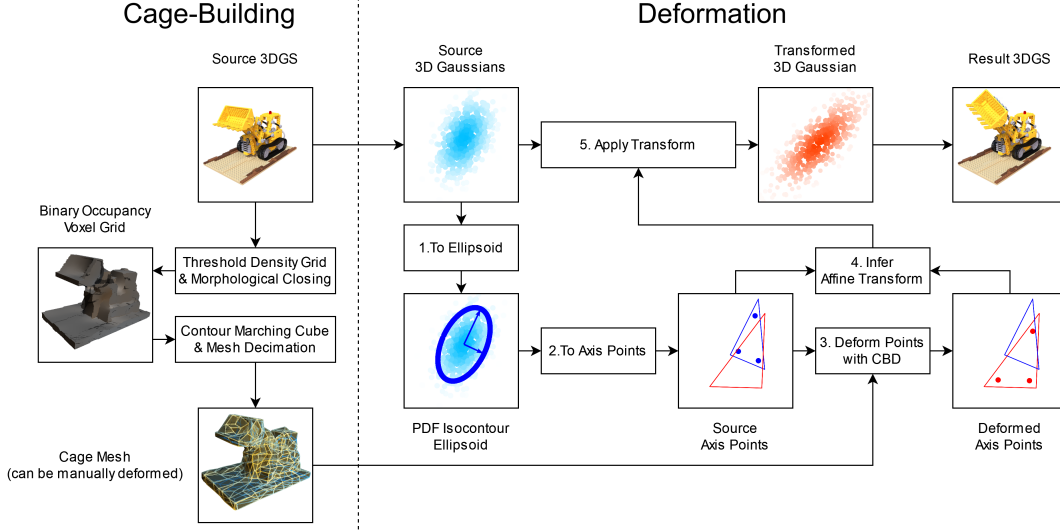


Fig. 2. Overview of our method. For cage-building, we convert the 3DGS representation into a binary occupancy grid, compute its morphological closing, and then mesh its contour and decimate it for the coarse cage mesh. For deformation, our method converts the gaussians in 3DGS into ellipsoids and further into proxy points (axis points in the diagram). The point clouds are deformed using cage-based deformation, and the changes in point clouds will be used to infer the transformation to apply to the gaussians. Note we plot the 2D variant of the deformation algorithm for ease of visualization.

$$\text{pdf}(\mathbf{x}) = (2\pi)^{-3/2} \det(\Sigma_d)^{-1/2} \exp\left(-\frac{1}{2}(\mathbf{x} - \mu_d)^T \Sigma_d^{-1} (\mathbf{x} - \mu_d)\right) \quad (4)$$

which can be rewritten as:

$$c_d = \frac{\text{pdf}(\mathbf{x})}{(2\pi)^{-3/2} \det(\Sigma_d)^{-1/2}}$$

$$Q_d = \frac{\Sigma_d^{-1}}{-2 \log c_d}$$

$$1 = (\mathbf{x} - \mu_d)^T Q_d (\mathbf{x} - \mu_d) \quad (5)$$

Compare Equation (5) to the quadric form of ellipsoid with mean \mathbf{v} and matrix \mathbf{A} :

$$(\mathbf{x} - \mathbf{v})^T \mathbf{A} (\mathbf{x} - \mathbf{v}) = 1 \quad (6)$$

It is found that Equation (5) can be seen as a quadric form of an ellipsoid with mean μ_d and matrix Q_d . This ellipsoid is the PDF isocontour of the original 3D Gaussian distribution at a given PDF value.

The isocontour ellipsoid's principal axes $p_i \in P_d$ and their length $s_i \in S_d$ can then be computed:

$$p_i = \text{Eigenvector}_i(Q_d) \quad (7)$$

$$s_i = \left(\frac{1}{\text{EigenValue}_i(Q_d)}\right)^{1/2} \quad (8)$$

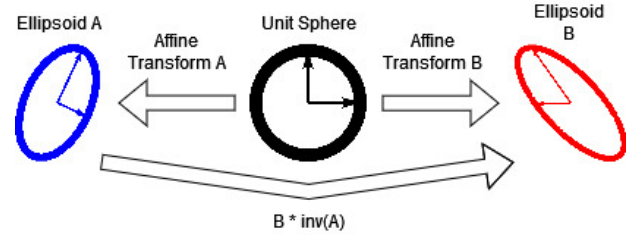


Fig. 3. Inferring affine transform from ellipsoids. Given two ellipsoids, A and B, both represented using affine transforms from the unit sphere. The transform that turns A to B is then BA^{-1} .

3.3.2 Ellipsoid To Axis Points. For the converted 3D ellipsoid d , given its center c_d , the principal axes $p_i \in P_d$, and their length $s_i \in S_d$. We can obtain three points on the ellipsoid $x_i \in X_d$ via:

$$x_i = c_d + p_i * s_i \quad (9)$$

Combined with the center point c_d , these four points SP_d (called axis points here) could represent an ellipsoid.

3.3.3 Deform Points with CBD. We then perform cage-based deformation on the axis points SP_d with source and target cages C_s and C_d . The resulting deformed axis points are referred to as DP_d .

3.3.4 Infer Affine Transform. Given the original and transformed axis points SP_d and DP_d , we then infer the affine transform that transforms the original distribution in the same way.

To begin with, all ellipsoids can be seen as unit spheres transformed by an affine transformation, where we rotate and scale the

principal axes of the unit sphere and then translate them to the ellipsoid center.

Since the principal axes of the unit sphere constitute an orthonormal base of the original space, stacking the transformed principal axes of the unit sphere as columns would give us the rotation and scaling matrix. The translation vector is the center of the ellipsoid.

For our axis point representation, the transformed principal axes can be acquired by calculating the vector difference between transformed on-surface points $x_{ddi} \in DP_d$ and the transformed center $c_{dd} \in DP_d$. The new center is the transformed center c_{dd} .

Therefore, the transform matrix T_B that would create the ellipsoid represented by DP_d is:

$$T_B = \begin{bmatrix} x_{dd1} - c_{dd} & x_{dd2} - c_{dd} & x_{dd3} - c_{dd} & c_{dd} \\ 0 & 0 & 0 & 1 \end{bmatrix} \quad (10)$$

The same could be done to SP_d , which produces the transform from unit sphere to the original ellipsoid T_A

As presented in Figure 3, given T_A and T_B , the transform T that turns source ellipsoid (A) to target ellipsoid (B) is:

$$T = T_B T_A^{-1} \quad (11)$$

Inferring and applying full affine transform is crucial to our method as this is how our method achieves scaling and rotation of gaussians.

3.3.5 Apply Transform. With the affine transform $T = \begin{bmatrix} R & t \end{bmatrix}$ that matches the deformation of cages inferred. We transform the 3D gaussian distribution using it:

$$\mu'_d = R\mu_d + t$$

$$\Sigma'_d = R\Sigma_d R^T$$

The covariance is then converted back into rotation and scaling by running singular value decomposition(SVD):

$$R'_d = \text{SVD}_U(\Sigma'_d)$$

$$S'_d = \text{sqrt}(\text{SVD}_\Sigma(\Sigma'_d))$$

where SVD_U and SVD_Σ represents the U and Σ in SVD.

4 EXPERIMENTS

4.1 Implementation Details

For cage building, the voxel grid’s resolution is set to 128; the density threshold is set to $1e-4$, and K is set to 16.

For deformation, we use 0.01 as the value of $\text{pdf}(\mathbf{x})$ to find PDF iso-contour ellipsoids. We use the mean value coordinate algorithm([Ju et al. 2005a]) for cage-based deformation. For cages that only encompass part of the scene, we only deform gaussians that fall within the cage’s convex hull for speed and stability.

4.2 Scene Editing

We showcase the deformation ability of our algorithm on scenes from the Synthetic NeRF [Mildenhall et al. 2020] dataset and the MipNeRF360[Barron et al. 2022] dataset. The cages are produced by our cage-building algorithm and then manually deformed.

The results are presented in Figure 1. It can be seen that our method achieves high-quality deformation on both synthetic and real-world captures. Our model supports deformation, simple transformation and enlarging of the selected object based on the cages.

4.3 Deformation Algorithm

To evaluate the deformation quality of our method, we conduct further experiments on scenes from the Synthetic NeRF[Mildenhall et al. 2020] and Synthetic NSVF[Liu et al. 2020] datasets. We employ the source and target cages from DeformingNeRF[Xu and Harada 2022] for standardizing comparison.

We compare our method with work that performs cage-based deformation on NeRF: DeformingNeRF[Xu and Harada 2022] and recent deformation methods using mesh-bounded 3DGS: SuGaR[Guédon and Lepetit 2023] and GaMeS[Waczyńska et al. 2024]. We deform the mesh in SuGaR and pseudo mesh in GaMeS using cage-based deformation via mean-value coordinates for equal comparison.

The results are presented in Figure 4. As can be seen, our method achieves comparable deformation quality against DeformingNeRF[Xu and Harada 2022], SuGaR[Guédon and Lepetit 2023] as well as GaMeS[Waczyńska et al. 2024].

The highlight of our method lies in achieving comparable quality while having other significant merits. This is presented in Table 1. Firstly, our method operates on the more efficient and capable 3D Gaussian Splatting[Kerbl et al. 2023] model. Therefore, we achieve higher rendering quality than DeformingNeRF; this can be seen from the zoomed-in views of Figure 4. Note the robot arm and toad belly in our method and GaMeS are much clearer and sharper than DeformingNeRF. Secondly, our model also directly deforms the underlying representation; therefore, no deformation is needed during rendering, unlike DeformingNeRF. Thirdly, unlike GaMeS and SuGaR, our method directly operates on the 3D gaussian distributions and does not change the underlying architecture of the method, making our model directly applicable to existing trained 3DGS representations without retraining. Finally, compared with SC-GS[Huang et al. 2023], our method does not require video data for learning deformation, so our method can operate on static scene captures while SC-GS cannot.

4.4 Cage-building Algorithm

To demonstrate the effectiveness of our cage-building algorithm, we apply it to scenes from the Synthetic NeRF[Mildenhall et al. 2020] dataset. We also compare the cage produced by our method against the pseudo mesh from GaMeS[Waczyńska et al. 2024] and the mesh from SuGaR[Guédon and Lepetit 2023]. For easier comparison, we manually removed the spurious parts of the SuGaR proxy mesh.

It can be seen from Figure 5 that our method constructs coarse cages that encompass the object and preserve its coarse geometry shape. Our coarse cage is simpler and thus easier to manipulate than the triangle soup from GaMeS or the dense mesh from SuGaR.

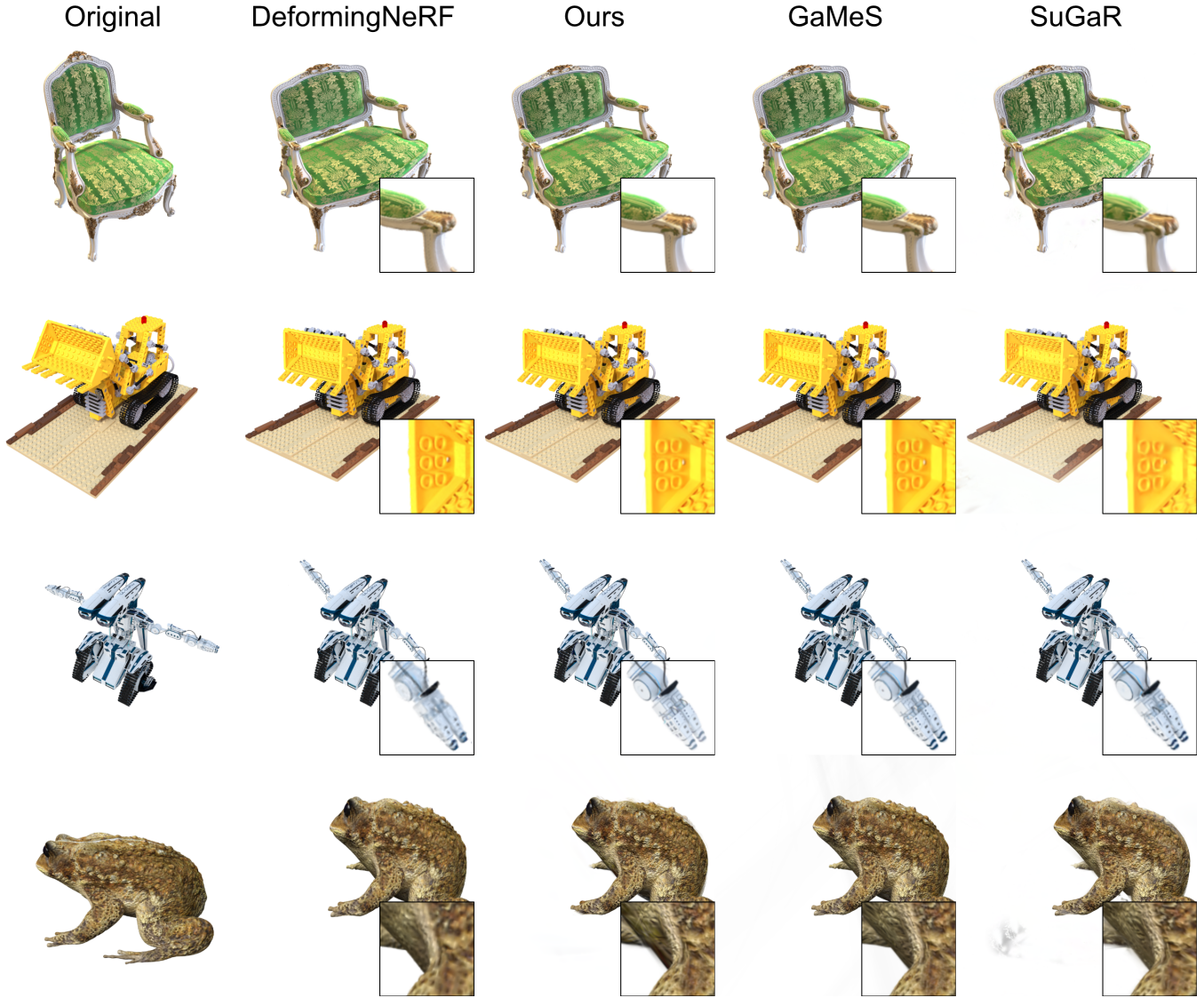


Fig. 4. Rendered view of the original scene and the deformed ones. We also provide zoomed-in views of the deformation results in the bottom-right corner. Our method produces results with quality comparable to DeformingNeRF, SuGaR and GaMeS despite operating on the more capable 3DGS and does not modify its architecture.

method	based-on	deform on render	changes model architecture	requires video data
Ours	3DGS	No	No	No
DeformingNeRF	NeRF	Yes	No	No
GaMeS	3DGS	No	Yes	No
SuGaR	3DGS	No	Yes	No
SC-GS	3DGS	No	No	Yes

Table 1. Other aspects about the compared methods, with the better option bolded. Our method is based on 3DGS and does not deform during rendering. Therefore, our method has a speed and quality advantage over NeRF-based methods. Our method does not alter 3DGS’s architecture, making our method directly applicable to existing trained 3DGS scenes without re-training. Our method can also perform deformation without video training data, which is required for SC-GS[Huang et al. 2023].

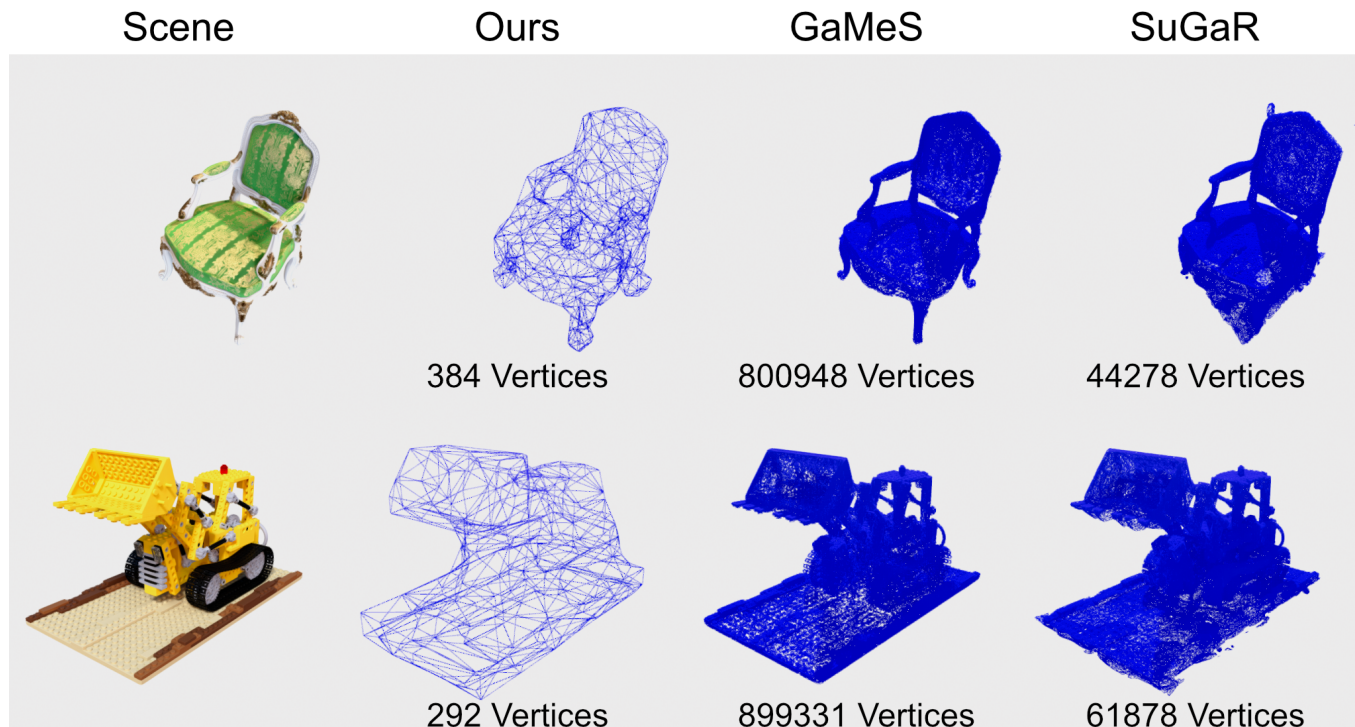


Fig. 5. Wireframe view of manipulation proxies, with their vertex count attached. We present and compare the cage produced by our algorithm against the proxy representation provided by other methods. It can be seen that the cage produced by our method is simpler and thus easier to deform compared with those of GaMeS or SuGaR.

4.5 Ablation Study

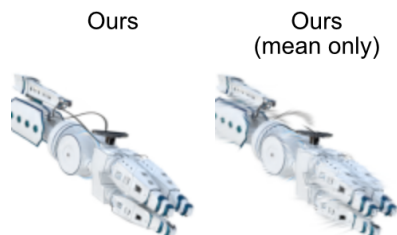


Fig. 6. Comparing our method against the naive mean-only baseline. Note that the wires on the robot arm in the mean-only baseline are blurry and jagged but not in our method.

To demonstrate the necessity of our method, namely the proxy point cloud and the affine transform trick in step 4. We compare our method against a naive variant of our algorithm where we only transform the mean of gaussians using cage-based deformation. We test this on the robot scene of the Synthetic NSVF dataset[Liu et al. 2020].

The zoomed-in results are presented in Figure 6. As can be seen, this naive method leads to significant deformation artifacts, such as the blurry and jagged wires on the arm of the robot. This is

because the mean-only variant does not handle rotation at all, while our method handles it by inferring the full affine transforms and applying them to the gaussians.

In this paper, we propose GSDeformer, a method that achieves free-form deformation on 3D Gaussian Splatting(3DGS) without changing its underlying architecture. Our approach extends cage-based deformation to 3DGS by converting 3DGS to a proxy point cloud representation whose deformation can be transferred to 3DGS, all without requiring any additional data or changes to 3DGS’s architecture. We also propose a complementary cage-building algorithm to automatically create the cages for deforming 3DGS.

Currently, our method, despite being mathematically well-grounded, cannot achieve deformation in real-time. A simpler and faster scheme would be a valuable next step. Transformation of color parameters, such as the spherical harmonics, should also be considered.

REFERENCES

- Jonathan T. Barron, Ben Mildenhall, Dor Verbin, Pratul P. Srinivasan, and Peter Hedman. 2022. Mip-NeRF 360: Unbounded Anti-Aliased Neural Radiance Fields. *CVPR* (2022).
- A. Blattmann, Tim Dockhorn, Sumith Kulal, Daniel Mendelevitch, Maciej Kilian, and Dominik Lorenz. 2023. Stable Video Diffusion: Scaling Latent Video Diffusion Models to Large Datasets. *ArXiv abs/2311.15127* (2023). <https://api.semanticscholar.org/CorpusID:265312551>
- Stéphane Calderon and Tamy Boubekeur. 2017. Bounding Proxies for Shape Approximation. *ACM Transactions on Graphics (Proc. SIGGRAPH 2017)* 36, 5, Article 57 (july 2017).
- Yiwen Chen, Zilong Chen, Chi Zhang, Feng Wang, Xiaofeng Yang, Yikai Wang, Zhong-gang Cai, Lei Yang, Huaping Liu, and Guosheng Lin. 2023. GaussianEditor: Swift

and Controllable 3D Editing with Gaussian Splatting. arXiv:2311.14521 [cs.CV]

Tony DeRose and Mark Meyer. 2006. Harmonic Coordinates.

Yutao Feng, Xiang Feng, Yintong Shang, Ying Jiang, Chang Yu, Zeshun Zong, Tianjia Shao, Hongzhi Wu, Kun Zhou, Chenfanfu Jiang, and Yin Yang. 2024. Gaussian Splatting: Dynamic Fluid Synthesis with Gaussian Splatting. arXiv:2401.15318 [cs.GR]

Michael S. Floater. 2003. Mean value coordinates. *Comput. Aided Geom. Des.* 20 (2003).

Lin Gao, Jie Yang, Bo-Tao Zhang, Jiali Sun, Yu-Jie Yuan, Hongbo Fu, and Yu-Kun Lai. 2024. Mesh-based Gaussian Splatting for Real-time Large-scale Deformation. *ArXiv abs/2402.04796* (2024).

Michael Garland and Paul S. Heckbert. 1997. Surface simplification using quadric error metrics. *Proceedings of the 24th annual conference on Computer graphics and interactive techniques* (1997). <https://api.semanticscholar.org/CorpusID:621181>

Antoine Guédon and Vincent Lepetit. 2023. SuGaR: Surface-Aligned Gaussian Splatting for Efficient 3D Mesh Reconstruction and High-Quality Mesh Rendering. *arXiv preprint arXiv:2311.12775* (2023).

Antoine Guédon and Vincent Lepetit. 2024. Gaussian Frosting: Editable Complex Radiance Fields with Real-Time Rendering. *arXiv preprint arXiv:2403.14554* (2024).

Yi-Hua Huang, Yang-Tian Sun, Ziyi Yang, Xiaoyang Lyu, Yan-Pei Cao, and Xiaojuan Qi. 2023. SC-GS: Sparse-Controlled Gaussian Splatting for Editable Dynamic Scenes. *arXiv preprint arXiv:2312.14937* (2023).

Clément Jambon, Bernhard Kerbl, Georgios Kopanas, Stavros Diolatzis, Thomas Leimkühler, and George Drettakis. 2023. NeRFshop: Interactive Editing of Neural Radiance Fields. *Proceedings of the ACM on Computer Graphics and Interactive Techniques* 6, 1 (May 2023). <https://repo-sam.inria.fr/fungraph/nefshop/>

Chenfanfu Jiang, Craig Schroeder, Joseph Teran, Alexey Stomakhin, and Andrew Selle. 2016. The material point method for simulating continuum materials. In *ACM SIGGRAPH 2016 Courses* (Anaheim, California) (SIGGRAPH '16). Association for Computing Machinery, New York, NY, USA, Article 24, 52 pages. <https://doi.org/10.1145/2897826.2927348>

Pushkar Joshi, Mark Meyer, Tony DeRose, Brian Green, and Tom Sanocki. 2007. Harmonic coordinates for character articulation. *ACM Trans. Graph.* 26, 3 (jul 2007), 71–es. <https://doi.org/10.1145/1276377.1276466>

Tao Ju, Scott Schaefer, and Joe Warren. 2005a. Mean value coordinates for closed triangular meshes. In *ACM Siggraph 2005 Papers*. 561–566.

Tao Ju, Scott Schaefer, and Joe D. Warren. 2005b. Mean value coordinates for closed triangular meshes. *ACM SIGGRAPH 2005 Papers* (2005).

Bernhard Kerbl, Georgios Kopanas, Thomas Leimkühler, and George Drettakis. 2023. 3D Gaussian Splatting for Real-Time Radiance Field Rendering. *ACM Transactions on Graphics* 42, 4 (July 2023). <https://repo-sam.inria.fr/fungraph/3d-gaussian-splatting/>

Shaouxi Li and Ye Pan. 2023. Interactive Geometry Editing of Neural Radiance Fields. *ArXiv abs/2303.11537* (2023).

Yaron Lipman, David Levin, and Daniel Cohen-Or. 2008. Green Coordinates. *ACM SIGGRAPH 2008 papers* (2008).

Lingjie Liu, Jiatao Gu, Kyaw Zaw Lin, Tat-Seng Chua, and Christian Theobalt. 2020. Neural Sparse Voxel Fields. *NeurIPS* (2020).

Miles Macklin, Matthias Müller, and Nuttapon Chentanez. 2016. XPBD: position-based simulation of compliant constrained dynamics. *Proceedings of the 9th International Conference on Motion in Games* (2016).

Ben Mildenhall, Pratul P. Srinivasan, Matthew Tancik, Jonathan T. Barron, Ravi Ramamoorthi, and Ren Ng. 2020. NeRF: Representing Scenes as Neural Radiance Fields for View Synthesis. In *ECCV*.

Ri-Zhao Qiu, Ge Yang, Weijia Zeng, and Xiaolong Wang. 2024. Feature Splatting: Language-Driven Physics-Based Scene Synthesis and Editing. *ArXiv abs/2404.01223* (2024). <https://api.semanticscholar.org/CorpusID:268819312>

Joanna Waczyńska, Piotr Borycki, Sławomir Tadeja, Jacek Tabor, and Przemysław Spurek. 2024. GaMeS: Mesh-Based Adapting and Modification of Gaussian Splatting. (2024). arXiv:2402.01459 [cs.CV]

Yuxuan Wang, Xuanyu Yi, Zike Wu, Na Zhao, Long Chen, and Hanwang Zhang. 2024. View-Consistent 3D Editing with Gaussian Splatting. *ArXiv abs/2403.11868* (2024).

Jing Wu, Jia Wang Bian, Xinghui Li, Guangrun Wang, Ian D Reid, Philip Torr, and Victor Adrian Prisacariu. 2024. GaussCtrl: Multi-View Consistent Text-Driven 3D Gaussian Splatting Editing. *ArXiv abs/2403.08733* (2024).

Chuhua Xian, Hongwei Lin, and Shuming Gao. 2009. Automatic generation of coarse bounding cages from dense meshes. *2009 IEEE International Conference on Shape Modeling and Applications* (2009), 21–27.

Tianyi Xie, Zeshun Zong, Yuxing Qiu, Xuan Li, Yutao Feng, Yin Yang, and Chenfanfu Jiang. 2023. PhysGaussian: Physics-Integrated 3D Gaussians for Generative Dynamics. *arXiv preprint arXiv:2311.12198* (2023).

Tianhan Xu and Tatsuya Harada. 2022. Deforming Radiance Fields with Cages. In *ECCV*.

Tianyuan Zhang, Hong-Xing Yu, Rundu Wu, Brandon Y. Feng, Changxi Zheng, Noah Snaveley, Jiajun Wu, and William T. Freeman. 2024. PhysDreamer: Physics-Based Interaction with 3D Objects via Video Generation. *arxiv* (2024).

Licheng Zhong, Hong-Xing Yu, Jiajun Wu, and Yunzhu Li. 2024. Reconstruction and Simulation of Elastic Objects with Spring-Mass 3D Gaussians. *arXiv preprint arXiv:2403.09434* (2024).

A DETAILED DESCRIPTION OF DEFORMATION ALGORITHM

We present an algorithmic description of the deformation algorithm in Algorithm 1. Note that CBD refers to the mean-value coordinate cage-based deformation algorithm, SVD stands for singular value decomposition $U\Sigma V = \text{SVD}(M)$

Algorithm 1 GSDeformer Deformation Algorithm

Require: 3DGS scene S_s , Source Cage C_s , Target Cage C_d , PDF threshold pdf(x).

Ensure: Deformed 3DGS scene S_d

$S_d = \text{Empty3DGS}()$

▷ for every gaussian in 3DGS ◀

for (opacity α , SH param C , mean μ , rot R , scale S) in S_s **do**

▷ 1.find PDF isocontour ellipsoid in quadric form μ and Q ◀

$$\Sigma = \text{RSSR}^T$$

$$c = \frac{\text{pdf}(\mathbf{x})}{(2\pi)^{-3/2} \det(\Sigma)^{-1/2}}$$

$$Q = \frac{\Sigma^{-1}}{-2 \log c}$$

▷ find ellipsoid's center c , principal axis p and their length s ◀

$$c = \mu$$

$$p = \text{EigenVector}(Q)$$

$$s = \left(\frac{1}{\text{EigenValue}(Q)} \right)^{1/2}$$

▷ 2. convert into axis points ◀

$$SP = [c]$$

for i in 1..3 **do**

└ $SP.append(c + p_i * s_i)$

▷ 3.deform axis points with CBD ◀

$$DP = \text{CBD}(SP, C_s, C_d)$$

▷ 4.infers affine transform ◀

$$T_A = \begin{bmatrix} SP_1 - SP_0 & SP_2 - SP_0 & SP_3 - SP_0 & SP_0 \\ 0 & 0 & 0 & 1 \end{bmatrix}$$

$T_B =$ same as above, but replace SP with DP

$$T = T_B T_A^{-1}$$

▷ 5. applies transform ◀

$$\begin{bmatrix} R & t \end{bmatrix} = T$$

$$\mu' = R\mu + t$$

$$\Sigma' = R\Sigma R^T$$

$$R' = \text{SVD}_U(\Sigma')$$

$$S' = (\text{SVD}_\Sigma(\Sigma'))^{1/2}$$

▷ write result ◀

$S_d.append(\text{opacity } \alpha, \text{ SH param } C, \text{ mean } \mu', \text{ rot } R', \text{ scale } S')$

return S_d
